International Journal of Remote Sensing

ISSN: 0143-1161 (Print) 1366-5901 (Online) Journal homepage: https://www.tandfonline.com/loi/tres20

Mangrove biomass carbon stock mapping of the Karimunjawa Islands using multispectral remote sensing

Pramaditya Wicaksono, Projo Danoedoro, Hartono & Udo Nehren

To cite this article: Pramaditya Wicaksono, Projo Danoedoro, Hartono & Udo Nehren (2016) Mangrove biomass carbon stock mapping of the Karimunjawa Islands using multispectral remote sensing, International Journal of Remote Sensing, 37:1, 26-52, DOI: 10.1080/01431161.2015.1117679

To link to this article: https://doi.org/10.1080/01431161.2015.1117679

INTERNATIONAL JOURNAL OF REMOTE SENSING, 2016
VOL. 37, NO. 1, 26–52
http://dx.doi.org/10.1080/01431161.2015.1117679

Taylor & Francis
Taylor & Francis Group

Mangrove biomass carbon stock mapping of the Karimunjawa Islands using multispectral remote sensing

Pramaditya Wicaksono[a,b], Projo Danoedoro[a], Hartono[a] and Udo Nehren[b]

[a]Cartography and Remote Sensing, Faculty of Geography, Universitas Gadjah Mada, Yogyakarta, Indonesia; [b]ITT, Cologne University of Applied Sciences, Cologne, Germany

ABSTRACT

Among vegetated coastal habitats, mangrove forests are among the densest carbon pools. They store their organic carbon in the surrounding soil and thus the sequestered carbon stays in the sediment for a long time and cannot be easily returned to the atmosphere. Additionally, mangroves also provide various important ecosystem services in coastal areas and surroundings. Accordingly, it is important to understand the distribution of biomass carbon stock in mangrove habitats in a spatial and temporal context, not only to reduce CO_2 concentrations in the atmosphere, but also for their sustainability. The objectives of this research are to map the mangrove carbon stock and estimate the total biomass carbon stock sheltered by mangrove forests, with the Karimunjawa Islands as a study site, using the widely available passive remote sensing system ALOS AVNIR-2. The modelling and mapping of mangrove carbon stock incorporates the integration of image pixel values and mangroves field data via empirical modelling. Vegetation indices and PC bands at different levels of radiometric corrections were all used as the input in the mangrove carbon stock modelling so that the effectiveness and sensitivity of different image transformations to particular radiometric correction levels could be analysed and understood. Afterward, the accuracy and effectiveness of each mangrove carbon stock-mapping routine was compared and evaluated. The accuracy of the best mangrove above-ground carbon stock (AGC) map modelled from vegetation index is 77.1% (EVI1, SE 5.89 kg C m^{-2}), and for mangrove below-ground carbon stock (BGC) it is 60.0% (GEMI, SE 2.54 kg C m^{-2}). The mangrove carbon stock map from ALOS AVNIR-2 PC bands showed a maximum accuracy of 77.8% (PC2, SE 5.71 kg C m^{-2}) and 60.8% (PC2, SE 2.48 kg C m^{-2}) for AGC and BGC respectively. From the resulting maps, the Karimunjawa Islands are estimated to shelter 96,482 tonnes C of mangroves AGC with a mean value of 21.64 kg C m^{-2} and 24,064 tonnes C of mangroves BGC with a mean value of 5.39 kg C m^{-2}. Potentially, there are approximately 120,546 tonnes C of mangrove biomass carbon stock in the Karimunjawa Islands. Remote-sensing reflectance can successfully model mangrove carbon stock based on the relationship between mangrove canopy properties, represented by leaf area index (LAI) and the tree or root biomass carbon stock. The accuracy of the mangrove carbon stock map is subject to errors, which are sourced mainly from: (1) the absence of a species-specific biomass allometric equation for several species present in the study area; (2) the

ARTICLE HISTORY
Received 7 January 2015
Accepted 28 October 2015

CONTACT Pramaditya Wicaksono prama.wicaksono@geo.ugm.ac.id

generalized standard conversion value of mangrove biomass to mangrove carbon stock; (3) the relationship between mangrove reflectance and mangrove LAI; (4) the relationship between mangrove reflectance and above-ground mangrove biomass and carbon stock due to its relationship with LAI; (5) the relationship between mangrove LAI and mangrove below-ground parts; (6) the inability to perform mangrove carbon stock modelling at the species level due to the complexities of the mangrove forest in the study area; (7) background reflectance and atmospheric path radiance that could not be completely minimized using image radiometric corrections and transformations; and (8) spatial displacement between the actual location of the mangrove forest in the field and the corresponding pixel in the image. The availability of mangrove biomass carbon stock maps is beneficial for carrying out various management activities, and is also very important for the resilience of mangroves to changing environments.

1. Introduction

Among vegetated coastal habitats, mangrove forests are one of the densest carbon pools (Nellemann et al. 2009). They allocate more biomass underground to support their existence in a muddy substrate than other species (Komiyama, Ong, and Poungparn 2008), and hence they store a large amount of underground carbon stock. Instead of using sequestered inorganic carbon simply for growth, they also store organic carbon in the surrounding soil. As a result, the sequestered carbon will remain in the sediment for a long time and it is not readily returned to the atmosphere. The ability of mangroves to store carbon in the sediment is called long-term carbon sequestration. The ability of vegetated coastal habitats, including mangroves, to perform long-term carbon sequestration is 10–50 times higher than terrestrial habitats (Laffoley and Grimsditch 2009; Nellemann et al. 2009). Additionally, mangroves also provide various important ecosystem services such as nursery grounds, maintenance of biodiversity, sheltering for fauna, sediment stabilization, coastal defence, and pollution filtering (Boonsong, Piyatiratitivorakul, and Patanaponpaiboon 2003; Nagelkerken et al. 2008; Wu et al. 2008). Accordingly, it is important to understand the distribution of biomass carbon stock in mangrove habitats in a spatial and temporal context, not only in reducing CO_2 concentrations in the atmosphere, but also for their sustainability.

Mangrove forests are currently decreasing at an alarming rate due to improper land use management. The development of agriculture, aquaculture, industry, settlement, infrastructure, and tourism in coastal areas are the key triggers. It is reported that 20% of mangroves have been lost since 1980, and from 2000 to 2005, 118 km^2 of mangrove forests were removed annually (FAO 2007). A massive loss of mangrove is not only a major loss in the availability of a highly potential carbon sink, but also problematic because it becomes a source of carbon in the atmosphere (Ong 2002; Granek and Ruttenberg 2008).

Understanding mangrove biomass is very useful in recognizing the interaction between vegetation, the stability of that interaction, and also the variation in

population numbers. Maps of mangrove biomass carbon stock are very important because they provide a better understanding of the spatio-temporal biomass and carbon dynamics. Despite this importance, quantitative information on mangrove biomass carbon stock is scarce. The spatio-temporal availability of continuous mangrove carbon stock data, which is very important for the mitigation of and adaptation to climate change, sustainable management of coastal areas and small islands, natural resources inventory, and conservation and rehabilitation, is currently missing at various scales and levels of user needs. These issues are mainly a result of the limited accessibility of mangrove areas, the cost effectiveness of field measurements, and the complexities of mangrove as an environmental system (Lu, Batistella, and Moran 2005; Bouillon et al. 2008).

The most common procedure for upscaling plot-level data to landscape level is spatial interpolation and extrapolation. Performing this procedure is problematic as the variation in carbon stock in a particular forest or landscape is assumed to be linear and only a function of the sampled plot data. In fact, variation in carbon stock may not be linear but strongly controlled by species abundance and landscape configuration. This procedure may only deliver a confident result when the number of samples adequately represents the variation of carbon stock in the field. However, the accuracy and precision of the resulting carbon stock information cannot be evaluated properly. Moreover, this analysis cannot be used to provide spatially continuous carbon stock data. Furthermore, during multi-temporal analysis, the use of extrapolated or interpolated data is ineffective since the location and type of the changing carbon stock cannot be identified. Therefore, in order to obtain a good spatial and temporal context of carbon stock distribution, field data must be integrated with remote-sensing data (Lu, Batistella, and Moran 2005; Kuenzer et al. 2011).

Critically important mangrove carbon stock information can only be obtained using remote sensing. The current developments in remote-sensing technology enable data to be acquired with higher spatial resolution, radiometric precision, spectral sensitivity, and temporal frequency. Furthermore, image-processing methods and efficient integration between remote sensing and field and laboratory data are becoming sophisticated. Remote-sensing approaches have been used to map mangrove biomass (Simard et al. 2006; Li et al. 2007; Fatoyinbo et al. 2008; Simard et al. 2008; Fatoyinbo and Armstrong 2010; Hamdan, Aziz, and Hasmadi 2014), tree height (Simard et al. 2006; Fatoyinbo et al. 2008), leaf area index (LAI) (Knyazikhin et al. 1999; Green and Mumby 2000; Chen et al. 2004; Potithep et al. 2009; Kuenzer et al. 2011; Kovacs et al. 2013), canopy structure (Mougin et al. 1999; Proisy et al. 2000, 2002; Lucas et al. 2007), and species composition (Vaiphasa, Skidmore, and de Boer 2006; Myint et al. 2008; Kamal and Phinn 2011; Wong and Fung 2014). Despite these advances, the use of passive remote-sensing systems for mangrove biomass carbon stock mapping has been very limited (Kuenzer et al. 2011). The logical framework behind the mapping, the most effective and suitable input data sets, the assumptions and limitations during mapping, the methodologies to map carbon stock, and the expected accuracy have not yet been clearly defined (Fatoyinbo et al. 2008). The available publications on remote sensing for mangrove carbon stock mapping (Fatoyinbo et al. 2008; Wicaksono et al. 2011) do not provide any explanation of the mapping framework, nor the most suitable methodological approach.

This article highlights the gap in knowledge of remote sensing for mangrove biomass carbon stock mapping. The objectives of this research are to map mangrove carbon stock and estimate the total biomass carbon stock sheltered by mangrove forests, using the Karimunjawa Islands as a study site. Most previous works on mangrove biomass carbon stock mapping were performed using active remote-sensing systems rather than the widely available passive systems (Fatoyinbo and Armstrong 2010; Hamdan, Aziz, and Hasmadi 2014). Although passive remote-sensing systems were used to model and map vegetation biomass in studies conducted by Lu, Batistella, and Moran (2005), Proisy, Couteron, and Fromard (2007), Wicaksono et al. (2011), Latifi, Fassnacht, and Koch (2012), Laurin et al. (2014), and Kattenborn et al. (2015), few used mangrove vegetation as the main object of interest (Proisy, Couteron, and Fromard 2007; Wicaksono et al. 2011). In this research, the use of passive and multispectral remote-sensing system is emphasized because these are readily available and more cost effective than hyperspectral data and active remote-sensing systems such as light detection and ranging (lidar). An ALOS AVNIR-2 (Advance Land Observation Satellite Advanced Visible and Near Infrared Radiometer type 2) image was used in this research to represent the passive multispectral remote-sensing system. In addition, when multispectral data can deliver accurate mangrove carbon stock maps, the future use of hyperspectral data for mangrove carbon stock mapping will deliver even better results. Hereafter, the term remote sensing refers to passive remote sensing.

2. Data and study areas

This study was conducted on Karimunjawa and Kemujan islands of the Karimunjawa Islands group (Figure 1). The Karimunjawa Islands are located in the Java Sea, a shallow marine environment located between Java and Kalimantan in Indonesia. The Karimunjawa Islands are located between 5°40′39″–5°55′0″ south and 110°05′57″–110° 31′15″ east. The Karimunjawa Islands have been under the authority of the Karimunjawa National Park since 1999 and are administered by the Indonesian Forestry Ministry (Decree of The Minister of Forestry (SK Menhut) No.78/Kpts-II/1999). Hence the mangroves in Karimunjawa are well protected. Mangroves in Karimunjawa are mainly located on the strait between the Karimunjawa and Kemujan islands. Mangrove forests in this area are very dense, and therefore on satellite images the two islands appear to be connected. Mangroves can also be found fringing the shoreline in the western and northern parts of Karimunjawa Island and in the central-southern parts of Kemujan Island. Mangroves also grow on other islands such as in Cemara Kecil Island, Krakal Besar Island, Krakal Kecil, and Sintok Island. Characterized by relatively low stands, mangroves in Karimunjawa are classified as oceanic mangroves. There are 24 true mangroves species from the orders Avicenniaceae, Cobretaceae, Euphorbiaceae, Meliaceae, Rhizophoraceae, Sonneratiaceae, Sterculiaceae, Rubiaceae, Acanthaceae, Palmae, and Myrsinaceae (Nababan et al. 2010).

The ALOS AVNIR-2 image of the study area was acquired on 10 October 2010, in the same year as the field data collection. As a result, the temporal bias and spatial displacement between field data and the corresponding image pixel values are minimal. ALOS AVNIR-2 has 10 m spatial resolution and three visible bands: blue (420–500 nm), green (520–600 nm), and red (610–690 nm), and a near-infrared band (760–890 nm).

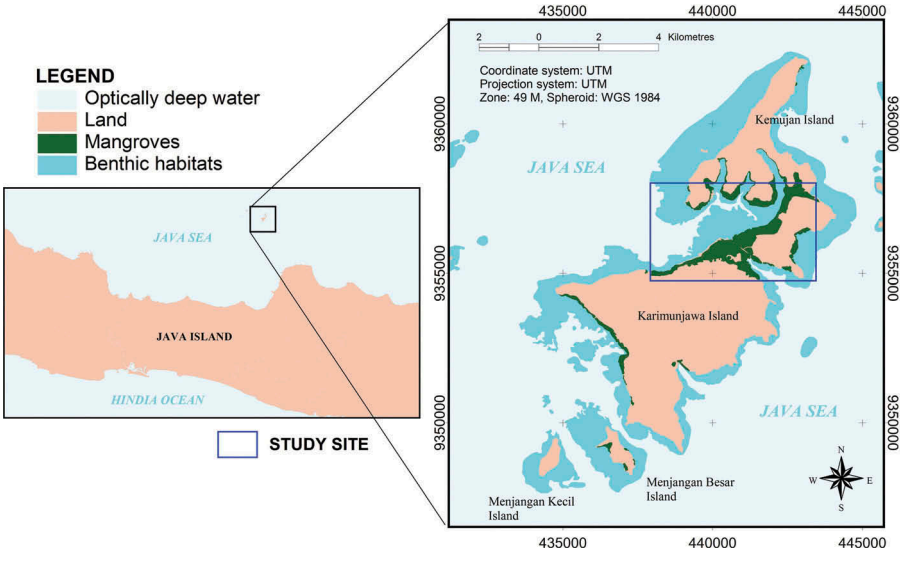

Figure 1. Study areas for mangrove carbon stock mapping in the Karimunjawa Islands.

ALOS AVNIR-2 images can be used to determine various vegetation indices (Table 2) and precise mapping up to the 1:25,000 scale.

3. Methods

3.1. *Field survey*

A mangrove field survey was conducted in May 2010. The stratified random aligned sampling method was used to assist in the selection of sample locations, using normalized difference vegetation index (NDVI) transformation and Isodata classification as the sampling mapping unit. NDVI was sliced at six regular intervals (0.1) starting from 0 to 0.53 (the maximum value of NDVI in the scene). The location of samples follows the sampling transects created perpendicular to the shoreline. The sampling transects were deliberately drawn to pass through mangroves with the highest sampling mapping unit variation in order to accommodate the differences in the condition of mangroves in the study area. The distance between transects varies accordingly. Mangrove samples were collected in different sampling mapping units passed by the transect. In each sampling mapping unit, the sample site was purposely located around the centre of the sampling mapping unit to accommodate the geolocation error of the ALOS AVNIR-2 image, as well as the error of the handheld GPS reading used to record the coordinates of mangrove samples.

A total of 40 spatially distributed mangroves samples were obtained, 25 of which were used to build a mangrove carbon stock model and 15 to test the accuracy of the resulting mangrove carbon stock map (Figure 2). In each sample, mangroves were separated into tree, poles, and saplings. Mangroves at the tree stage were sampled at 400 m^2, poles at 100 m^2, and saplings at 25 m^2. 'Tree' refers to any stand with a diameter at breast height (DBH) >20 cm, 'pole' refers to a young stand with DBH 10–20 cm, and

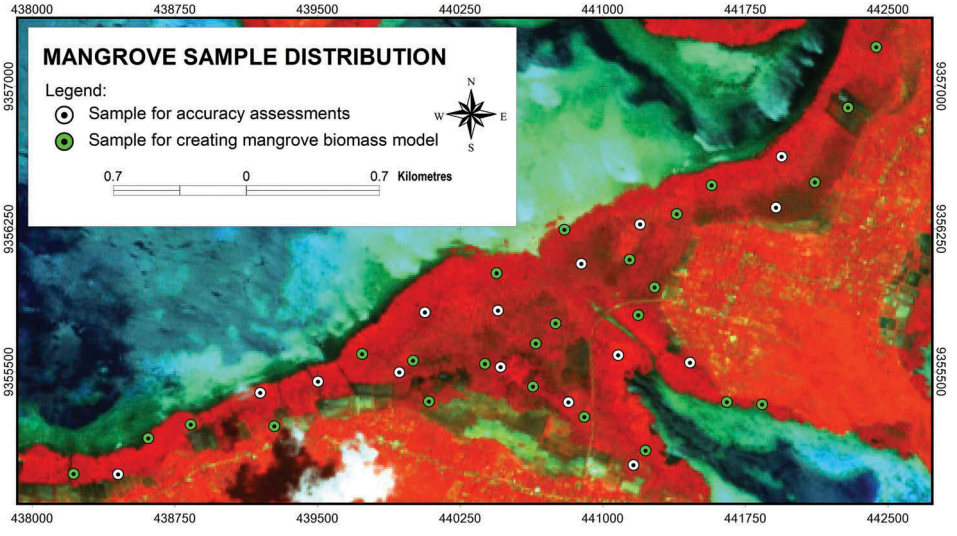

Figure 2. Mangrove sample distribution overlaid on a 4,3,2 (near-infrared, red, green) RGB colour composite of ALOS AVNIR-2.

'sapling' refers to any stand mangroves with a height of 1.5 m and DBH of up to 10 cm. Tree DBH, diameter of tree at the height of the lowest living branch (DB), tree height, and species composition were measured individually for each stand. Stem wood density for different mangroves species was adopted and compiled from literature reviews (Martawijaya et al. 1992; Worldagroforestry 2013). A total of 916 mangrove stands were measured. In order to have common measurement units between these growth stages, the value of biomass was standardized to tonnes per hectare.

Mangrove above- (AGB) and below-ground biomass (BGB) were calculated individually for each stand using allometric equations. Above-ground parts consisted of stem, branches, and leaves, while below-ground parts were the roots. The concept behind allometric equations is that the proportion of growth in one part is similar to that in others, which means that the diameter of the tree is correlated to its weight (Shinozaki et al. 1964; Oohata and Shinozaki 1979; Komiyama, Poungparn, and Kato 2005). Therefore, because obtaining information about mangrove biomass does not require harvesting it is non-destructive. This method is environmentally friendly, time and cost effective, and requires less effort than others. Thus, more samples can be obtained. This is the most suitable field method for obtaining mangrove samples for remote-sensing modelling.

Five mangrove species were measured using species-specific allometric equations (Table 1). The biomass of the remainder of the mangrove species was calculated using common allometric equations (Komiyama, Poungparn, and Kato 2005). For *Rhizopora apiculate* alone, the biomass of prop roots was also measured and was added to the value of BGB. Next, mangrove above- (AGC) and below-ground carbon stock (BGC) were obtained using the conservative estimate of 0.494 g C g^{-1} biomass (Murdiyarso et al. 2009). D_{max} is the upper range of mangrove DBH for the corresponding mangrove biomass allometric equation. Thus, the corresponding allometric equation only works

Table 1. Species-specific biomass allometric equation for mangrove found in the Karimunjawa Islands.

No	Species	Biomass Allometric Equation (kg)		Sources
		Above ground	Below ground	
1	*Avicennia marina*	$0.308(DBH)^{2.11}$ D_{max} = 35 cm	$1.28(DBH)^{1.17}$ D_{max} = 35 cm	Comley and McGuinness (2005)
2	*Xylocarpus granatum*	$0.0823(DBH)^{2.59}$ D_{max} = 25 cm	$0.145(DBH)^{2.55}$ D_{max} = 8 cm	Clough and Scott (1989) Poungparn et al. (2002)
3	*Bruguiera gymnorrhiza**	$0.186(DBH)^{2.31}$ D_{max} = 25 cm	–	Clough and Scott (1989)
4	*Rhizopora apiculata**	$0.235(DBH)^{2.42}$ D_{max} = 28 cm	$0.00698(DBH)^{2.61}$ D_{max} = 28 cm $W_{stilt} = 0.0209(DBH)^{2.55}$	Ong, Gong, and Wong (2004)
5	*Rhizopora stylosa**	–	$0.261(DBH)^{1.86}$ D_{max} = 15 cm	Comley and McGuinness (2005)

W_{stilt} = Prop root weight of *Rhizopora apiculata*
DBH = Diameter at breast height (cm) (*for *Rhizophoraceae* DBH is measured 30 cm above roots)
D_{max} = Upper range of mangrove DBH for the corresponding mangrove biomass allometric equation

effectively in estimating mangrove biomass with DBH lower than the specified D_{max}. Finally, the carbon stock of each mangrove stand was summed to obtain the total mangrove AGC and BGC in each sample.

Common allometric equations used to estimate mangrove AGB and BGB were developed by Komiyama, Poungparn, and Kato (2005), using the static model of plant form by Oohata and Shinozaki (1979) as the basis. Mangrove wood density and tree DBH are required using the allometric approach of Komiyama et al. Wood density values are dependent on species type, growth conditions, and vegetation parts measured, hence becoming a species control parameter in the common allometric equation. The use of wood density makes the common allometric equation work like a species-specific allometric equation. These required variables are also used in the common allometric equations developed by Chave et al. (2005). Biomass allometric equations from Komiyama, Poungparn, and Kato (2005) were preferred because these were developed using mangroves in Southeast Asia, which are considered representative of mangroves in the Karimunjawa Islands. The common allometric equations used to obtain mangrove AGB and BGB are as follows:

$$\text{Above Ground Biomass (kg)} = 0.251p(\text{DBH})^{2.46}; D_{max} = 49\,\text{cm}, \quad (1)$$

$$\text{Leaf Biomass (kg)} = 0.135p(\text{DB})^{1.696}; D_{max} = 49\,\text{cm}, \quad (2)$$

$$\text{Below Ground Biomass (roots) (kg)} = 0.199p^{0.899}x(\text{DBH})^{2.22}; D_{max} = 45\,\text{cm}, \quad (3)$$

p = wood density of the corresponding mangrove species (kg m^{-3}), DBH = diameter of tree at breast height (cm), DB = diameter of tree at the height of the lowest living branch (cm).

3.2. *Image correction*

The ALOS AVNIR-2 image was corrected geometrically in order to minimize spatial displacement between image pixels and the corresponding location in the field.

Coordinates taken from the Worldview-2 image of Karimunjawa and Kemujan islands were used as the ground control points (GCPs) for geometric correction. The GCPs were not taken from the topographic map of the Karimunjawa Islands because its geometric accuracy is inadequate. Second-order polynomial transformation was used to accommodate the number of GCPs and tvariation in the topography of the Karimunjawa Islands. For the interpolation method, nearest neighbour was preferred so that the original pixel values of the image could be maintained.

Radiometric corrections covered the conversion from DN to spectral radiance, and spectral radiance to both sensor and surface reflectance. The coefficients for radiance conversion were taken from the image header. The sensor reflectance image was obtained using the standard procedure for ALOS AVNIR-2 reflectance conversion as described in Sakuno et al. (2007). The band-averaged solar spectral irradiance (ESUN) values were also adapted from Sakuno et al. (2007). The surface reflectance image was derived by removing path radiance from the sensor reflectance image. Path radiance in the image was removed using the dark subtraction method (Armstrong 1993; Hadjimitsis et al. 2010). Pixels of cloud shadows over optically deep water were used as the dark targets.

3.3. *Mapping mangrove distribution*

Mangrove distribution or absent–present mapping was performed via visual interpretation of the standard false-colour composite image (4,3,2). This colour composite emphasizes the contrast and boundary between mangroves and other land covers. Mangroves appear as deep red in comparison to the brighter red of other vegetation cover. A map of mangrove distribution was used in building a mangrove mask image to mask out non-mangrove pixels. This mask image was necessary to isolate mangrove pixels during principal component analysis (PCA). Masking out non-mangrove pixels will increase the capabilities of PCA transformation to maximize the variation in the feature space, and thus the resulting PC bands provide better information on variation in mangrove characteristics.

Ideally, mangrove carbon stock should be mapped at the species level. Mangrove species mapping has been successfully carried out using passive remote-sensing systems (Vaiphasa, Skidmore, and de Boer 2006; Myint et al. 2008; Kamal and Phinn 2011). However, in this research, mapping mangrove carbon stock at the species level was not feasible because a mangrove species map could not be obtained, due to the complexity of mangrove species composition in the study area. Based on field surveys, there are 22 different classes of mangrove species in the study area. The number of samples for each class is inadequate as the training area, and in the accuracy assessments during digital classification. Thus, mangrove carbon stock mapping was only performed at the community level.

3.4. *Image transformation*

3.4.1. *Vegetation indices*

The most common image transformation used to model and map mangroves is the vegetation index, which has been widely and extensively used to map and model vegetation properties (Van der Meer et al. 2000; Huete et al. 2002; Thenkabail et al. 2002; Jiang et al.

Table 2. Vegetation indices used to model mangrove carbon stock using ALOS AVNIR-2. ρ is reflectance and the subscript is the wavelength region; thus green, red, and blue are the wavelengths equivalent to those colours, NIR is near-infrared and rb is a combination of red and blue bands, which is required to render the ARVI index atmospherically resistant. The value of γ is set to 1 due to the non-availability of an aerosol model in the study area.

No	Index	Algorithm	Coefficients	References
1	SR	$\frac{\rho_{red}}{\rho_{NIR}}$	–	Birth and McVey (1968) Schlerf, Atzberger, and Hill (2005)
2	DVI	$\rho_{NIR} - \rho_{red}$	–	Richardson and Everitt (1992)
3	NDVI	$\frac{\rho_{NIR} - \rho_{red}}{\rho_{NIR} + \rho_{red}}$	–	Edwards (2004) Huete et al. (2002) Kiage and Walker (2009) Rouse et al. (1973)
5	ARVI	$\frac{(\rho_{NIR} - \rho_{rb})}{(\rho_{NIR} + \rho_{rb})}$ Where $\rho_{rb} = \rho_{red} - \gamma(\rho_{blue} - \rho_{red})$	$\gamma = 1$	Kaufman and Tanre (1992) Liu et al. (2004)
7	VARI	$\frac{(\rho_{green} - \rho_{red})}{(\rho_{green} + \rho_{red} - \rho_{blue})}$	–	Gitelson et al. (2002) Viña and Gitelson (2011)
9	TVI	$\frac{1}{2}(120(\rho_{NIR} - \rho_{green})) - 200(\rho_{red} - \rho_{green})$	–	Broge and Leblanc (2000) Wamunyima (2005)
10	EVI1	$G\frac{\rho_{NIR} - \rho_{red}}{\rho_{NIR} + (C1 \times \rho_{red}) - (C2 \times \rho_{blue}) + L}(1 + L)$	$C1 = 6$ $C2 = 7.5$ $L = 1$ $G = 2.5$	Huete et al. (2002)
11	EVI2	$2.5 \times \left(\frac{\rho_{NIR} - \rho_{red}}{\rho_{NIR} + (2.4 \times \rho_{red}) + 1}\right)$	–	Jiang et al. (2008)
12	MSARVI	$\frac{2\rho_{NIR} + 1 - \sqrt{\left[(2\rho_{NIR} + 1)^2 - \gamma(\rho_{NIR} - \rho_{rb})\right]}}{2}$	–	Huete et al. (1992) Huete and Liu (1994)
13	GEMI	$GEMI = \eta(1 - 0.25\eta) - \left(\frac{\rho_{red} - 0.125}{1 - \rho_{NIR}}\right)$ Where $\eta = \frac{2(\rho_{NIR}{}^2 - \rho_{red}{}^2) + 1.5\rho_{NIR} + 0.5\rho_{red}}{\rho_{NIR} + \rho_{red} + 0.5}$	–	Pinty and Verstraete (1992) Van Der Meer et al. (2000)

Note: SR, simple ratio; DVI, difference vegetation index; VARI, visible atmospherically resistant index; MSARVI, modified soil and atmospherically resistant vegetation index; TVI, triangular vegetation index; EVI, enhanced vegetation index; EVI2, enhanced vegetation index-2; GEMI, global environment monitoring index.

2008; Eitel et al. 2008; Viña and Gitelson 2011; Wicaksono et al. 2011). Each vegetation index has a different sensitivity to different vegetation biophysical and biochemical properties such as LAI, canopy cover, chlorophyll and nitrogen content, vegetation fragment, biomass, and carbon stock. In this study, several vegetation indices were selected based on simplicity, input bands, and robustness (Table 2). Simple vegetation indices include SR, NDVI, and DVI; indices that rely heavily on visible bands include atmospherically resistant vegetation index (ARVI), VARI, and MSARVI; robust indices include TVI, EVI, EVI2, and GEMI. These vegetation indices have self-correction abilities such as normalizing the variation in background soil reflectance, atmospheric disturbance, and biomass variation.

3.4.2. *PCA*

PCA has been used on data from passive remote-sensing systems to successfully model vegetation biomass in different types of forest (Patel and Majumdar 2010; Wicaksono et al. 2011; Kattenborn et al. 2015). The aim in applying PCA during mangrove carbon stock mapping was to obtain a component that can explain the

variation in mangrove carbon stock. PCA produces a component that consists of information from several input bands, and hence it is more effective than using an individual spectral band. PCA has the ability to accentuate object-intrinsic information, separating noise from useful information, and when applied to pixels of a particular object (e.g. mangrove pixels) the resulting PC bands will provide the variation within the mangroves, which may be due to species composition or biochemical/biophysical properties. In this study, PCA was run using covariance and a correlation matrix to understand the effect of data normalization during PCA. During PCA transformation, the mangrove mask was applied to mask out non-mangrove pixels.

3.4.3. *Mangrove carbon stock modelling*

LAI is a function of leaf size, leaf number, and leaf layers per unit area, and is thus the main component that interacts with downwelling irradiance. Therefore, mangrove reflectance is a function of mangrove LAI, and other factors such as the composition of photosynthetic and protective pigments, leaf internal structures, leaf turgidity, leaf layers per unit area, and leaf spatial arrangement. Based on the allometric concept, mangrove LAI is correlated with the abundance of other mangrove parts. This statement is justified by the fact that mangrove leaf biomass can be estimated from tree height, wood density, and DB (Komiyama, Poungparn, and Kato 2005). Therefore, since mangrove biomass and carbon stock are also a function of wood density, DBH, and height, they are also correlated to LAI. As a result, mangrove carbon stock modelling and mapping can be performed directly.

The use of passive remote-sensing data to model and map mangrove biophysical properties incorporates the integration of image pixel values and mangrove field data via empirical modelling and physical model approaches, such as radiative transfer models (Atzberger 2004; Williams 2012). Regression analysis was mostly used to model and map mangrove carbon stock. Wicaksono et al. (2011) mapped mangrove carbon stock using regression analysis using vegetation indices, images of fraction endmember, and field biomass data. Biomass and carbon stock mapping in terrestrial ecosystems was also performed using regression analysis by calibrating image pixel values and field biomass carbon stock data (Thenkabail et al. 2002; Bajracharya 2008; Clark et al. 2011; Laurin et al. 2014; Kattenborn et al. 2015). Several empirical models of mangrove biophysical properties were reviewed by Kuenzer et al. (2011).

In this research study, vegetation indices and PC bands at different levels of radiometric correction were used as input in mangrove carbon stock modelling. Therefore, the effectiveness of and sensitivity of different image transformations to particular radiometric correction levels could be analysed and understood. The accuracy of the mangrove carbon stock map was assessed using the standard error of estimates (SE). The value of SE was converted to percentage error relative to the field data using a 95% confident level (95% CL). This kind of accuracy assessment produced the minimum and maximum possible accuracies of the predicted mangrove AGC and BGC model within 95% CL (Wicaksono et al. 2011). A research flowchart of mangrove carbon stock mapping is shown in Figure 3.

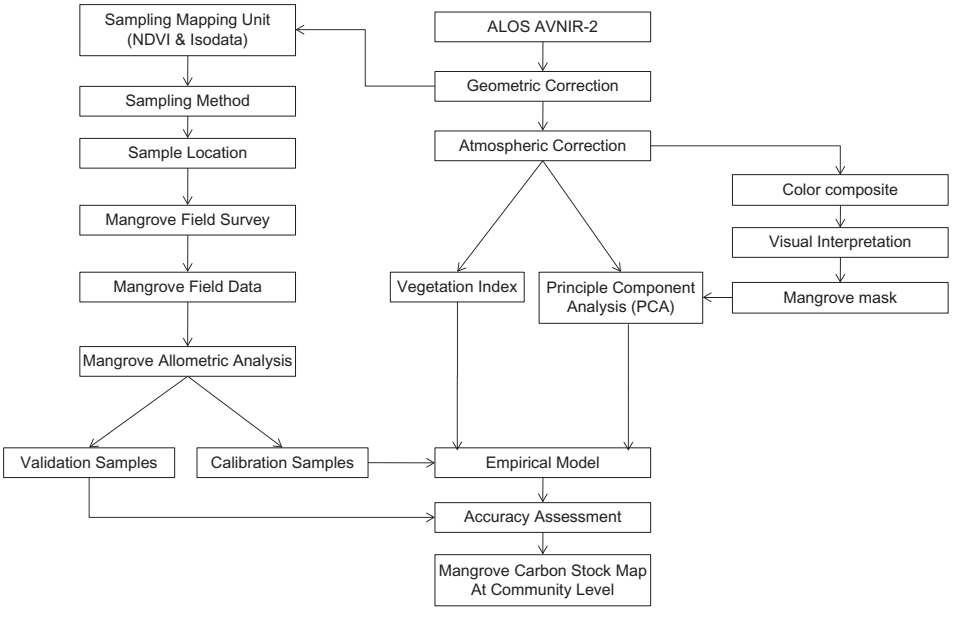

Figure 3. Flowchart of mangrove carbon stock mapping using passive remote-sensing system ALOS AVNIR-2.

4. Results and discussion

4.1. *Vegetation indices*

The performance of GEMI, EVI1, DVI, and TVI was almost identical in the modelling of mangrove AGC and BGC (Figure 4). For mangrove AGC modelling, R^2 (coefficient of determination) values for these four vegetation indices ranges between 0.650 and 0.690. EVI1 is slightly better than GEMI and DVI. The difference in R^2 between EVI1 and DVI and between GEMI and DVI was only 0.002. The accuracy of the mangrove AGC map modelled from EVI1 is 77.1% (SE 5.89 kg C m^{-2}), followed by GEMI (76.5%, SE 6.01 kg C m^{-2}) and DVI (76.2%, SE 6.11 kg C m^{-2}). For mangrove BGC, GEMI produced the best map (60.0%, SE 2.54 kg C m^{-2}), followed by DVI (59.4%, SE 2.58 kg C m^{-2}) and TVI (58.9%, SE 2.61 kg C m^{-2}). MSARVI yielded high R^2 for mangrove AGC modelling only at the surface reflectance level. The performance of MSARVI was not very good at the DN and sensor radiance levels; it was similar to GEMI, EVI1, EVI2, and DVI only at the reflectance level. This occurred because MSARVI utilizes several visible bands in its formula. Since visible bands are highly influenced by atmospheric scattering, full atmospheric correction is necessary to effectively use visible bands in the MSARVI formula. Therefore, MSARVI was only effective at the reflectance level where various factors such as sun illumination and path radiance were normalized. In contrast, GEMI, EVI1, EVI2, DVI – and sometimes NDVI – can be used directly at the DN level to produce an accurate mangrove carbon stock model. DVI, which is the simplest vegetation index, performed consistently across various radiometric correction levels. In addition to its consistency, the accuracy of the mangrove carbon stock map derived from DVI was mostly one of the best. DVI

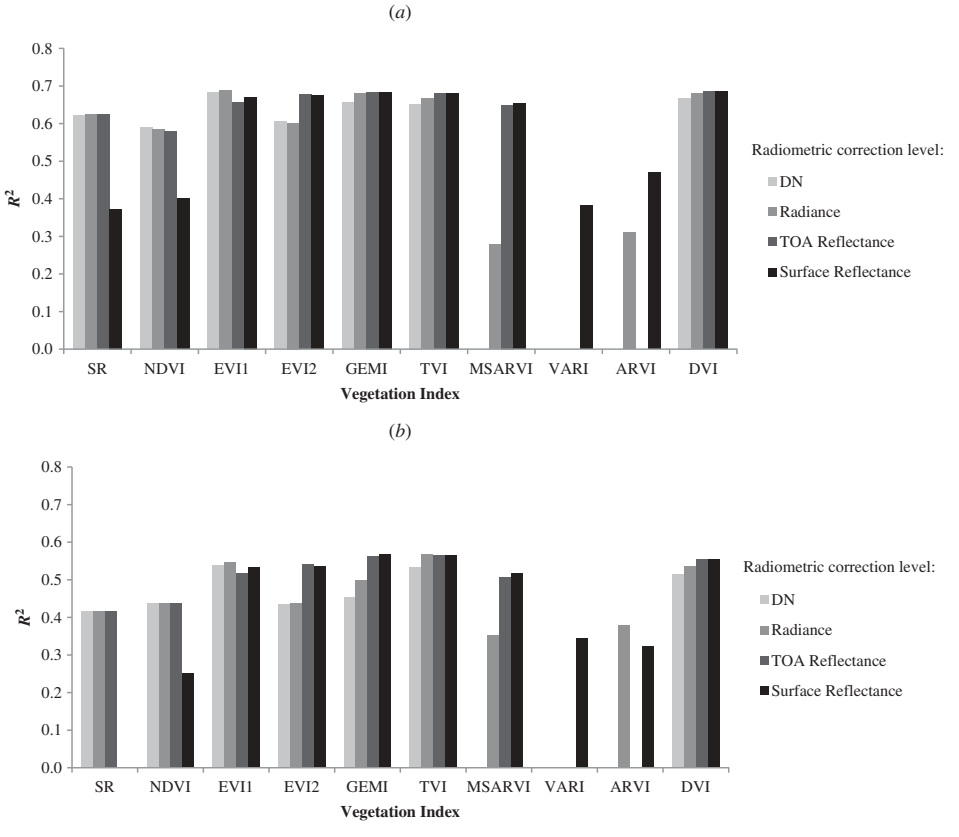

Figure 4. Results of vegetation index-based mangrove biomass carbon stock modelling using ALOS AVNIR-2 at different levels of radiometric correction: (*a*) above-ground carbon stock; (*b*) below-ground carbon stock. Vegetation indices reliant on visible bands such as VARI, ARVI, and MSARVI are very sensitive to the level of radiometric correction. VARI attained a significant value for R^2 with mangrove biomass carbon stock only when using surface reflectance data. On the other hand, ARVI produced a significant value of R^2 with mangrove biomass carbon stock using both sensor radiance and surface reflectance data. MSARVI did not produce a significant value of R^2 using DN.

was found to be the most effective vegetation index because: (1) the formula is simple; (2) the formula requires only the red and NIR bands and can thus be applied to most available passive multispectral images; and (3) the performance is consistent across various radiometric levels and improves with the application of radiometric correction. NDVI, as the most commonly used vegetation index, is only an average performer and is at the same level as SR.

Vegetation indices based on visible bands, such as VARI, ARVI, and MSARVI, were not very good in modelling mangrove carbon stock, most failing to yield significant R^2 using DN and radiance levels. At the reflectance level, only MSARVI produced higher R^2 than SR or NDVI. ARVI and VARI required full atmospheric correction, their performance being only average and hence they were the worst performers. This highlights the weakness in using a visible band-based vegetation index for vegetation mapping. Atmospheric scattering in the visible bands should be corrected prior to applying a vegetation index formula. Furthermore, a vegetation index that relies solely on visible bands is

not recommended. This is shown by VARI, for example, which fully utilizes visible bands with no infrared band and is the worst performer. MSARVI and ARVI that include the NIR band have a higher R^2 than VARI. In contrast to the visible bands-based vegetation index that requires full atmospheric correction, the performance of SR and NDVI was worst at the surface reflectance level. The optimal R^2 yielded by SR and NDVI was obtained using DN or radiance level. NDVI and SR may be sensitive to either the atmospheric correction method or the dark targets used to generate the atmospheric offsets, although further research needs to be done to validate this statement. However, similar results were also obtained by Wicaksono et al. (2011) when using Landsat-7 ETM+ data to map mangrove carbon stock. In that study, NDVI and SR produced higher accuracy and lower standard error on images using DN and at the sensor radiance level.

GEMI, DVI, EVI1, EVI2, and TVI are the indices that best mapped mangrove carbon stock. The R^2 of these indices was beyond the upper range of the 95% confidence intervals to the mean. Sorted by the most consistent index, the ranking would be DVI > GEMI > EVI1 > EVI2 > TVI. DVI performance was consistently good at the DN, radiance, and reflectance levels. Thus, DVI can be applied with no radiometric corrections and thereby accelerates the process of mangrove carbon stock mapping. When several aspects such as consistency, time effectiveness, and accuracy were considered, DVI was found to be the most effective vegetation index. Nevertheless, the application of radiometric correction is recommended as it improves the overall accuracy of the resulting carbon stock map. The best carbon stock map was generated from an atmospherically corrected image. The results of carbon stock mapping using vegetation indices are summarized in Table 3. Maps of mangrove AGC and BGC with the highest accuracy are shown in Figures 5 and 6.

4.2. *PCA*

The quality of the mangrove carbon stock model acquired from ALOS AVNIR-2 PC bands increased with the application of radiometric correction. Generally, the quality of the carbon stock model derived from PC bands at DN was the lowest; sometimes R^2 was not significant, while that from PC bands at the reflectance level were the highest. At the DN level, mangrove pixel values in the blue band are as high as in the NIR band. Since mangroves have high chlorophyll and LAI, healthy reflectance in visible bands will never be higher than in the NIR band. In addition, the reflectance of mangroves in the blue and red bands should be low, and as a result both bands should have a positive correlation. However, at the DN level, the reflectance of mangrove in the blue band is

Table 3. Summary of mangrove carbon stock mapping using vegetation indices applied to ALOS AVNIR-2 image.

Mangrove carbon stock	Radiometric level	Index	Highest accuracy equation	R^2	SE (kg C m^{-2})	Accuracy (%)
AGC	Sensor radiance	EVI1	−376.29(EVI1)-75.146	0.688	5.89	77.1
BGC	Surface reflectance	GEMI	310.64(GEMI)-122.01	0.567	2.54	60.0
Mangrove carbon stock	Radiometric level	Index	Most consistent accuracy equation	R^2	SE (kg C m^{-2})	Accuracy (%)
AGC	Surface reflectance	DVI	2723.8(DVI)-234.11	0.686	6.11	76.2
BGC	Surface reflectance	DVI	623.54(DVI)-49.74	0.554	2.58	59.4

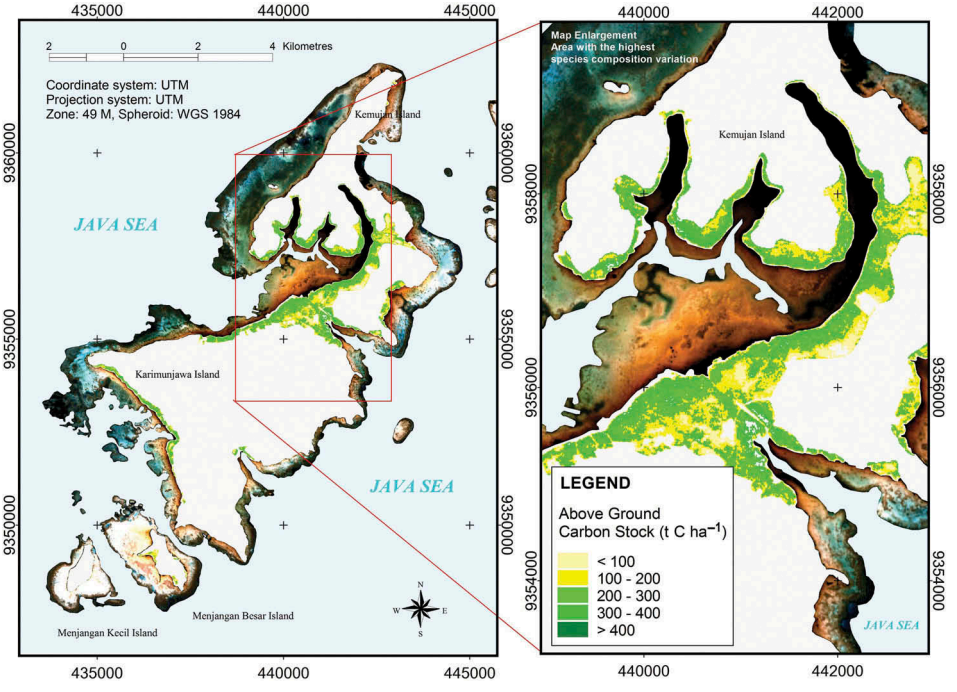

Figure 5. Mangrove AGC map derived from ALOS AVNIR-2 EVI1 (77.1%, SE = 5.89 kg C m^{-2}).

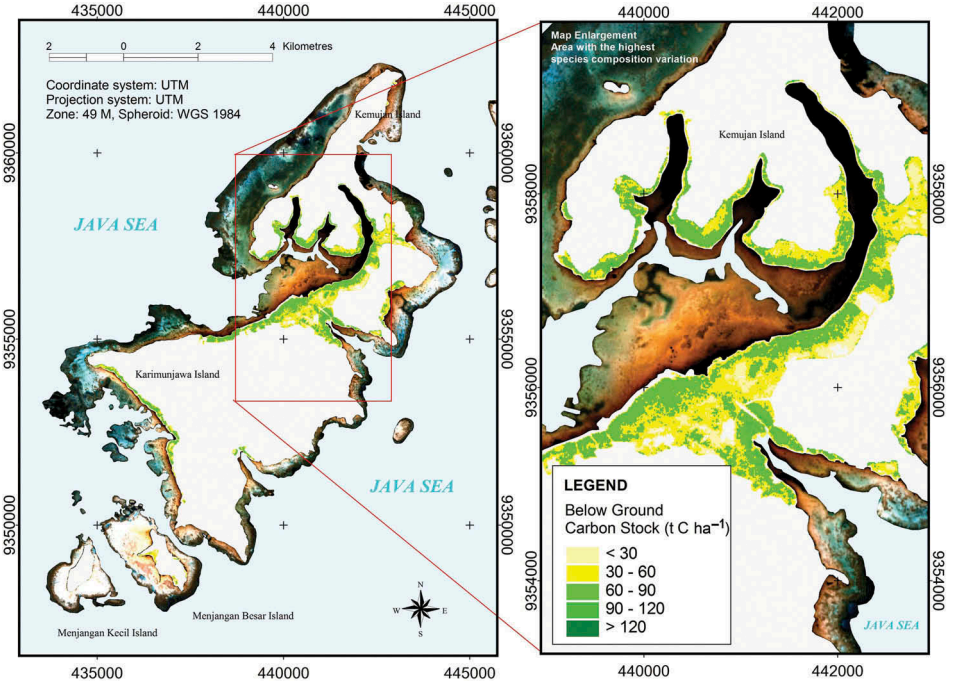

Figure 6. Mangrove BGC map derived from ALOS AVNIR-2 GEMI (60.0%, SE = 2.54 kg C m^{-2}).

higher than in the NIR band, and consequently, the relationship of reflectance between bands becomes unclear. These conditions were critical for the construction of covariance or the correlation matrix during PCA transformation. This altered band-to-band relationship affects the distribution and the variation of information in each PC band.

At surface reflectance, the variation in pixel values due to sunlight, atmospheric disturbances, and sensor configurations was normalized. Mangrove reflectance in the visible bands is much lower than in the NIR band, and thus a negative correlation between these bands can be expected in the creation of PC bands. Therefore, the relationship of mangrove reflectance among spectral bands consistently represents the actual condition of mangroves in the field. As a result, the quality of mangrove carbon stock model increased. The results of mangrove carbon stock modelling based on PC bands at various levels of radiometric corrections are provided in Figure 7.

The PC bands used for mangrove carbon stock modelling were derived from covariance and correlation matrices. Both matrices were evaluated to identify the effect of variance normalization in explaining the variation in mangrove carbon stock. The analysis showed that the accuracy of mangrove carbon stock map modelled from PC bands of both matrices did not differ greatly. The main difference between them was the performance of each PC band. At covariance matrix-based PC bands, only PC1 has the ability to model mangrove carbon stock. The model built from the remaining PC bands failed to obtain a significant relationship with mangrove carbon stock, mainly because most of the important mangrove information from input bands was concentrated on PC1. Hence, there were not enough variations in the later PC bands. Since the covariance matrix-based PCA transformation was running on non-normalized data variation, the eigenvalue of PC1 was very high because the first component extended effectively within the data space and hence it covered most of the available information from input spectral bands. In contrast, several ALOS AVNIR-2 PC bands derived from the correlation matrix were able to model mangrove carbon stock with high R^2. Interestingly, while PC2–4 successfully modelled mangrove carbon stock, none of the correlation matrix-based PC1 bands did so. During PCA transformation using correlation matrix, the data space was normalized and tighter; as a result, the first component only covered the most general mangrove information. Since mangrove carbon stock is recognized and considered as intrinsic and unique information, it is put into the later PC bands (PC2, PC3, PC4, etc.). The modelling results from Landsat-7 ETM+ using both matrices also showed that mangrove carbon stock was better modelled by PC2 or PC3 as opposed to PC1 (Wicaksono et al. 2011).

The mangrove carbon stock map from ALOS AVNIR-2 PC bands achieved a maximum accuracy of 77.8 and 60.8% for AGC and BGC, respectively. These accuracies refer to the SE of 5.71 kg C m^{-2} for AGC and 2.48 kg C m^{-2} for BGC. Results of mangrove carbon stock modelling using PCA are summarized in Table 4, and the resulting mangrove carbon stock maps are shown in Figures 8 and 9.

4.3. *Estimated mangrove carbon stock*

Mangroves with higher carbon stock are distributed near the shoreline of the eastern and western parts of the forest (Figures 5, 6, 8 and 9). The western parts include *Rhizopora apiculata, Rhizopora stylosa*, and *Scyphiphora hydrophyllacea* (200–400 tonnes C ha^{-1}), while the eastern parts are dominated by *R. apiculata, R. stylosa, S.*

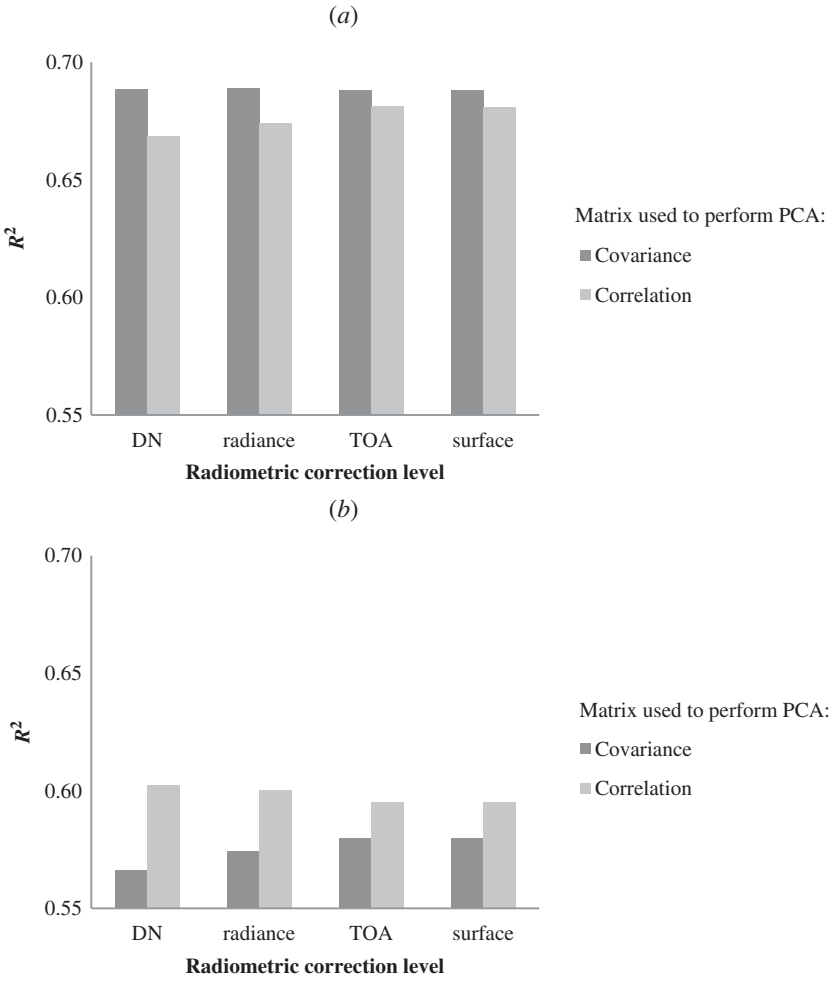

Figure 7. Mangrove carbon stock modelling using ALOS AVNIR-2 PC bands derived from both covariance and correlation matrix at various radiometric correction levels: (*a*) above-ground carbon stock, (*b*) below-ground carbon stock.

Table 4. Results of mangrove carbon stock mapping using ALOS AVNIR-2 PC bands.

Mangrove carbon stock	Radiometric level	Highest accuracy equation	R^2	PC	SE (kg C m^{-2})	Accuracy (%)
Covariance matrix						
AGC	Sensor radiance	9.4221(PC1)+202.12	0.689	PC1	5.83	77.3
	Surface reflectance	2856.4(PC1)+202.2	0.688	PC1	5.79	77.5
BGC	TOA reflectance	711.36(PC1)+50.019	0.580	PC1	2.53	60.2
	Surface reflectance	668.06(PC1)+50.015	0.580	PC1	2.53	60.2
Correlation matrix						
AGC	TOA reflectance	−3278(PC2)+202.42	0.681	PC2	5.72	77.8
	Surface reflectance	−3077.9(PC2)+202.43	0.681	PC2	5.71	77.8
BGC	DN	−1.6104(PC2)+49.959	0.603	PC2	2.48	60.8
	Surface reflectance	−733.08(PC2)+49.961	0.595	PC2	2.51	60.6

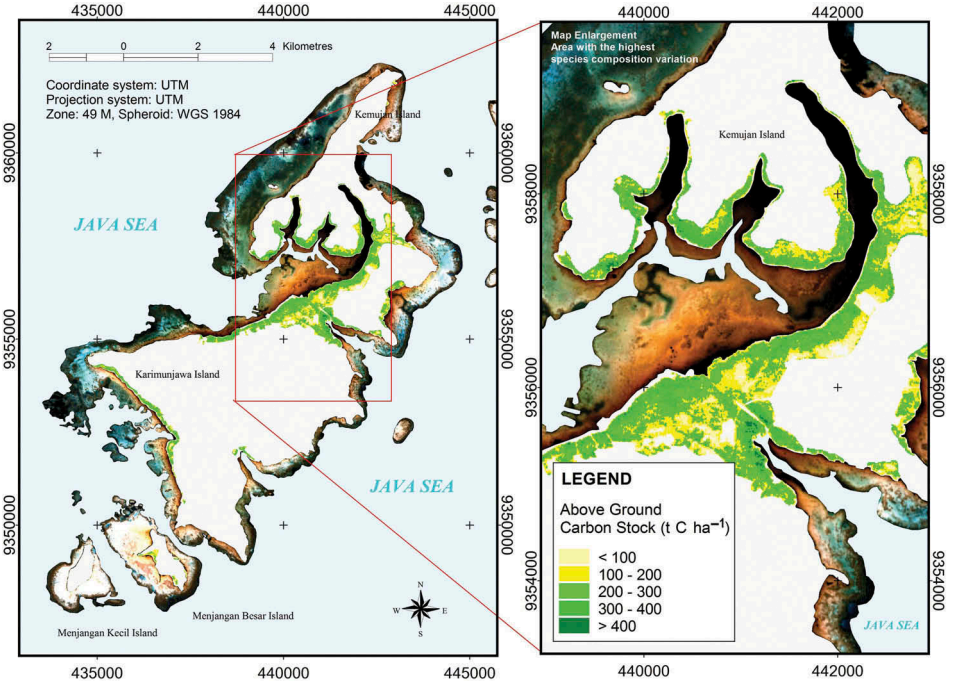

Figure 8. Mangrove AGC map modelled from ALOS AVNIR-2 PC2 of correlation matrix-based PCA with 77.8% (SE = 5.71 kg C m^{-2}).

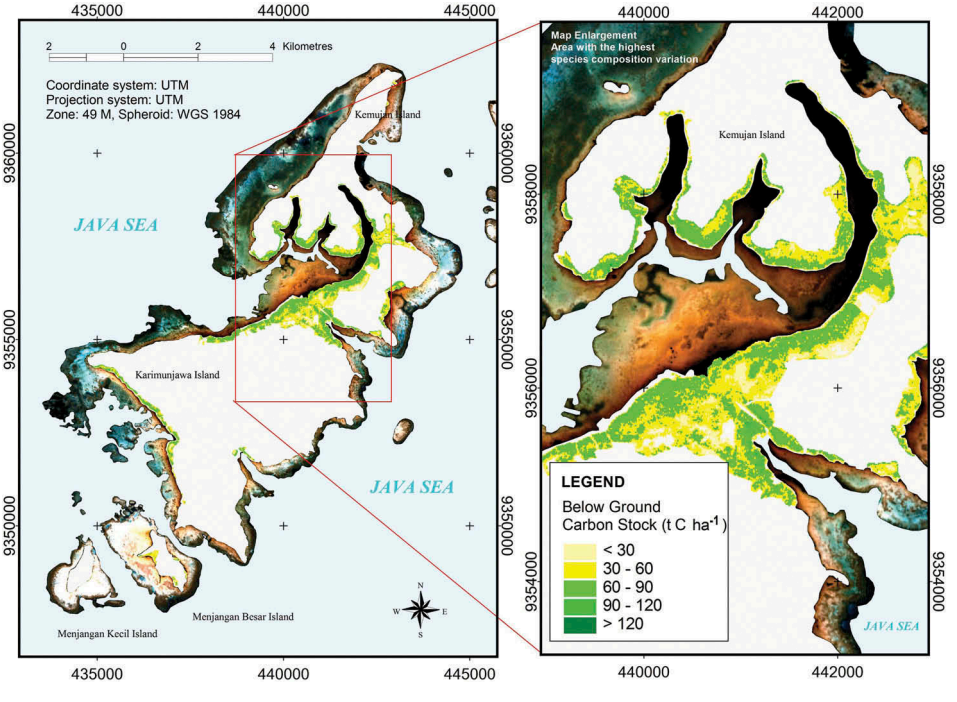

Figure 9. Mangrove BGC map modelled from ALOS AVNIR-2 PC2 of correlation matrix-based PCA with 60.8% accuracy (SE = 2.48 kg C m^{-2}).

hydrophyllacea, Ceriops tagal, and some clusters of *Bruguiera gymnorrhiza* (200 to >400 tonnes C ha^{-1}). The interior of the mangrove forest stores smaller amounts of carbon stock (0–300 tonnes C ha^{-1}), especially in areas near settlements, paddy fields, and fish ponds, and the northern parts of the main local road. In these areas, the most dominant species are *Excoecaria agallocha* and *C. tagal*.

The mangrove carbon stock in the study area is mainly controlled by the environmental conditions of the mangrove habitat, as in other natural forests. Human activities play an insignificant role in the variation in mangrove carbon stock since the forest is protected by the National Park. Previously, before protection by the Karimunjawa National Park was enforced, local people cut mangroves only for shipbuilding, and to some extent for constructing houses (based on interviews with the locals). Nevertheless, the scale of logging was small and did not significantly alter the natural composition of the forest. Consequently, the estimation of mangrove carbon stock in Karimunjawa can be used as a rough estimate of the amount of carbon stock in other mangrove forests of natural oceanic type.

The total mangrove carbon stock across the Karimunjawa and Kemujan islands can be estimated from the resulting maps. There are 96,482 tonnes of mangroves AGC with a mean value of 21.64 kg C m^{-2}, while BGC incorporates 24,064 tonnes C with the mean value of 5.39 kg C m^{-2}. This study shows that mangroves in the Karimunjawa and Kemujan islands store a huge amount of carbon stock, which should be protected. Potentially, there are approximately 120,546 tonnes C of mangrove biomass carbon stock in these two islands. The destruction of this ecosystem would potentially release a massive amount of CO_2 into the atmosphere, thus increasing the concentration of greenhouse gases (Ong 2002; Granek and Ruttenberg 2008; Nellemann et al. 2009).

4.4. *Mapping mangrove using passive remote-sensing systems*

Due to its suitable climatic and environmental conditions, Indonesia has an abundance of mangrove forests. Therefore, comprehensive and quantitative information about mangrove biomass carbon stock across Indonesia is required. At present, the availability of such data is scarce. For instance, the eastern areas of Indonesia have extensive areas of mangrove forests, but these areas are difficult to access for conducting extensive and regular field data collection. Accessibility limitations may lead to an ineffective field-based data collection. Remote sensing is the best alternative to overcome the aforementioned issues of mangrove carbon stock data collection.

Compared to passive remote sensing-systems, active systems are more frequently used to identify the characteristics of, and change in, mangrove forests (Lucas et al. 2007; Kuenzer et al. 2011). Mougin et al. (1999) studied mangrove forest backscattering using multi-frequency and multi-polarization radar. The polarimetric radar response by mangrove forest has been identified and interpreted to help in understanding mangrove canopy structure (Proisy et al. 2000, 2002). Polarimetric radar was also used to model and map mangrove biomass and carbon stock (Li et al. 2007; Fatoyinbo et al. 2008). Biomass estimation was also conducted by modelling tree or forest height using lidar (Clark et al. 2011; Latifi, Fassnacht, and Koch 2012) or other active remote-sensing data, such as the Shuttle Radar Topographic Mission (SRTM)

(Simard et al. 2006, 2008; Fatoyinbo and Armstrong 2010) and Tandem-X (Kattenborn et al. 2015). Unfortunately, excepting SRTM, these data sets are not widely available and thus it is difficult to replicate their work for faster and wider user needs.

Passive multispectral remote-sensing systems are currently still the better option for mapping at various levels of complexity and to meet different needs. Despite their availability and cost, passive hyperspectral systems have many spectral advantages compared with multispectral data, so they can potentially deliver a more accurate mangrove carbon stock map. The different wavelengths of passive remote-sensing systems provide unique spectral information that can be used to estimate and explain the variation in vegetation canopies. The complex interaction between downwelling irradiance and vegetation canopy may facilitate mapping of vegetation biophysical properties such as stand volume, tree height, and biomass carbon stock (Thenkabail et al. 2002; Patel and Majumdar 2010; Kuenzer et al. 2011; Wicaksono et al. 2011; Kattenborn et al. 2015). The possibility of mapping mangrove carbon stock is dependent on the extent of the relationship between its biophysical characteristics, especially with parts that directly interact with downwelling irradiance.

From a remote-sensing perspective, biomass, carbon stock, tree height, and stand volume are not directly related to mangrove reflectance (Woodhouse et al. 2012; Kattenborn et al. 2015). Downwelling irradiance only interacts with mangrove canopies before being either reflected, absorbed, or transmitted. Therefore, mangrove reflectance is actually a function of its canopy variation, which can be represented by LAI. LAI, which represents leaf number, leaf arrangement, and the amount of photosynthesizing tissue, affects the photosynthetic capacity of mangrove. Since the organic carbon stored within mangrove biomass is derived mainly from photosynthesis, LAI is a good indicator for quantifying vegetation carbon stock.

To successfully model mangrove carbon stock using remote-sensing approaches, the relationship between mangrove canopy properties (i.e., LAI, leaf biomass, and tree or root biomass carbon stock) must be known. These relationships were justified in the mangrove leaf and tree biomass allometric equation of Komiyama, Poungparn, and Kato (2005). Mangrove leaf biomass can be estimated from wood density and DB (Komiyama, Poungparn, and Kato 2005). Accordingly, leaf biomass is strongly correlated to the biomass of branch, stem, or root components. As a consequence, LAI, which is also a property of leaf biomass, is strongly correlated with tree biomass and carbon stock and thus mangrove reflectance can be used to model mangrove carbon stock.

The accuracy of the mangrove BGC map is lower than that of AGC because the BGC value was generated from a set of relationship among the mangrove above-ground tree biophysical properties. Furthermore, since the above-ground parts of mangrove biomass are related to leaves as the reflecting tissue, below-ground parts should be correlated as well. However, various errors from the relationships among tree properties entered the relationship between reflecting tissue (LAI) and mangrove BGC. As a result, the R^2 value of the regression analysis between mangrove pixel values and mangrove BGC decreased. Consequently, the accuracy of the mangrove BGC map is lower than that of the AGC map.

It is important to consider the variation in mangrove biophysical properties caused by species uniqueness, which is shown by inclusion of the species-specific mangrove wood

density in the common biomass allometric equation. Therefore, ideally, mangrove species mapping should be performed prior to the empirical modelling of mangrove biomass carbon stock. However, mangrove species mapping is a difficult task, even when using hyperspectral data, when the mangroves are very heterogeneous (Jusoff 2006; Kamal and Phinn 2011). Previous work by Myint et al. (2008) successfully mapped three mangrove types using object-based image analysis (OBIA) and lacunarity analysis on Landsat data. A multi-level of segmentation scale approach was applied to differentiate water bodies at the most general level of scale, to differentiate three types of mangrove forest (*Rhyzophora, Malaleuca*, and *Nypa*) at the fifth level. This approach yielded very high accuracy (94.2%) compared with of per-pixel classification algorithms (62.8%). Vaiphasa, Skidmore, and de Boer (2006) also managed to obtain a significant improvement in accuracy in mangrove species mapping using ASTER data after integrating soil pH spatial information in a post-classifier. Kamal and Phinn (2011) evaluated the performance of three mapping techniques, linear spectral unmixing (LSU), spectral angle mapper (SAM), and OBIA to map mangrove species using CASI-2 data. OBIA mapped four types of mangrove species (closed *Avicennia*, closed *Ceriops*, closed *Rhizopora*, open *Avicennia*) with 76% overall accuracy.

Compared to the aforementioned studies, the main factors that limited the use of ALOS AVNIR-2 image to map mangrove species in our study area were the complexities of mangrove species composition in the forest and the availability of field reference data. In previous studies, it was possible to generalize the variation of mangrove species composition into three (Myint et al. 2008) or four groups (Kamal and Phinn 2011) of forest types. Moreover, the forest has a clear mangrove zonation, where each sample plot is dominated by single mangrove species (Vaiphasa, Skidmore, and de Boer 2006). Mangrove field reference data in previous studies were also abundant, either from secondary data obtained from the corresponding authority, previous works, or existing vegetation floristic maps (Myint et al. 2008; Kamal and Phinn 2011). Therefore, the mapping could be effectively performed.

In contrast, the mangroves in our study area are still pristine and categorized as primary forest with various species combined in a single landscape unit, and there is no clear mangrove species zonation. Each sample consists of several species of relatively similar abundance. Only four samples were dominated by one mangrove species: one sample of low-density *R. stylosa*, two of low-density *R. apiculata*, and one of high-density *B. gymnorrhiza*. Almost all samples consisted of mixed species and it was impossible to create a working species classification scheme for digital image classification in regard to mangrove species mapping. There were 22 possible mangrove species composition classes.

It may be possible to generalize these 22 mangrove species classes into broader classes of forest type (i.e. *Rhizopora, Bruguiera, Ceriops, Excoecaria*, and *Scyphipora*. However, this approach would not be effective since each forest type actually consists of a mixed species. Since there was no unique species differentiation, performing mangrove carbon stock modelling based on these forest types will be no different than modelling at the community level. As a consequence, mangrove carbon stock mapping was not performed at the species level.

There were two main inputs used to model mangrove biomass in this research, vegetation indices and PC bands. Vegetation indices, namely EVI, DVI, and GEMI,

produced the better and most consistent mangrove carbon stock model. Among these indices, DVI is the most effective to model mangrove carbon stock. The best mangrove AGC and BGC maps were produced from PC bands, and the best map from PC bands was slightly more accurate than the best map from vegetation indices. Performing mangrove carbon stock mapping using PC bands is also more effective because it does not require any input other than the statistics of the image itself. Therefore, it can be applied to any image. Moreover, its effectiveness improves with increase in spectral bands and the application of radiometric correction. Increase in the number of input spectral bands during PCA transformation will also improve the information contained in each resulting PC band. Both correlation and covariance matrices can be used. Depending on the matrix used to generate the PC bands, PC1 is not necessarily the best component to model mangrove carbon stock. Since mangrove carbon stock is an intrinsic biophysical property, the best component to detect carbon stock variation might be PC2, PC3, or PC4. Nevertheless, regardless of variation in accuracy, the pattern of mangrove carbon stock spatial distribution from PC bands and vegetation indices is similar.

Other studies that utilized PC bands to model vegetation biomass also produced similar results. For instance, the results of the present study are in accord with those coherent of Kattenborn et al. (2015), where the application of PCA improved the quality of forest biomass modelling. The accuracy of biomass estimation modelled from PC3 of transformed Hyperion data was comparable to that of the canopy height model (CHM) of the Tandem-X and Worldview-2 systems. The present study also showed that forest biomass characteristics information is not contained in PC1. Instead, PC3 was found to be the best forest biomass predictor (R^2 = 0.566). Similarly, in this study, correlation matrix-based PC2 produced the best accuracy, slightly higher than that of the PC1-based mangrove biomass model from covariance matrix-based PCA (Table 4).

Future research into mangrove biomass carbon stock mapping should integrate passive and active remote-sensing data for higher accuracy, wider applicability, and data continuity. Passive remote-sensing systems may be adversely impacted by cloud cover and haze, and thus to fill in the missing data, active remote-sensing systems (i.e. synthetic aperture radar (SAR), lidar, is a good alternative. In addition, active remote-sensing systems can provide surface elevation data that can be used to estimate tree height for deriving the biomass (Clark et al. 2011; Latifi, Fassnacht, and Koch 2012; Laurin et al. 2014; Kattenborn et al. 2015). It is also important to perform a similar study in different mangrove habitats (i.e. deltaic mangroves, mangroves at different geographical locations, and mangroves with different species composition) so that the maximum descriptive resolution of passive multispectral remote-sensing systems to map mangroves biomass carbon stock can be better understood.

Finally, the available mangrove biomass carbon stock maps will be beneficial for carrying out various management activities. These include determining protected zones, assisting the process of mangrove conservation, setting the baseline for natural resource inventory, and evaluating management impacts (Green and Mumby 2000; Kuenzer et al. 2011). Mangrove carbon stock maps can be used to estimate mangrove biomass growth using multi-temporal data (Wicaksono et al. 2011). Biomass growth is a function of photosynthetic rate, which shows the amount

of CO_2 sequestered from the atmosphere. The sequestered CO_2 is converted into organic carbon for biomass growth. Multi-temporal analysis of mangrove data may reveal the changes occurring over time because the vegetative growth of mangrove can be directly observed above ground. Any change in the standing carbon stock or biomass can significantly modify the spatial and spectral properties of mangrove pixels. Mangrove carbon stock information in a spatial and temporal context is also very important for future adaptation to, and mitigation of, climate change and the resilience of mangrove to changing environments. Mangrove should receive even more credit for its environmental value and subsequent protection.

5. Conclusions

In conclusion, passive multispectral remote-sensing systems can be used to model mangrove biomass carbon stock. In this study using ALOS AVNIR-2 images, maps of mangrove AGC and BGC were created from vegetation indices and PC bands. The best mangrove AGC model from vegetation indices was produced by EVI1 with R^2 = 0.688, equal to SE of 5.89 kg C m^{-2} and 77.1% accuracy. The best mangrove BGC model was obtained by GEMI (R^2 = 0.567, SE = 2.54 kg C m^{-2}, 60.0% accuracy). An interesting finding is the good accuracy and consistency of simple DVI across radiometric correction levels. PCA produced a slightly higher accuracy than vegetation indices and was the best AGC model obtained in this study, with R^2 = 0.681, which is equal to SE of 5.71 kg C m^{-2} and 77.8% accuracy. PC2 produced the most accurate BGC model, with R^2 = 0.603, equal to SE of 2.48 kg C m^{-2} and 60.8% accuracy. These accuracies were obtained by PC2 and are comparable to the results from hyperspectral data and CHM from active remote-sensing systems in other studies. The success of using PC bands to model mangrove biomass is dependent on the ability of PCA transformation to aggregate information from input bands, accentuate unique information from mangrove pixels, separate noise, and reduce information redundancy. The accuracy of the mangrove biomass carbon stock map is subject to error, mainly from: (1) allometric estimation used to derive mangrove biomass above and below ground from tree DBH, DB, wood density, and tree height; and the absence of a species-species biomass allometric equation for most mangrove species found in the study area; (2) the standard conversion value of mangrove biomass to carbon stock; (3) the relationship between mangrove reflectance and reflecting tissue (LAI); (4) the relationship between mangrove reflectance and above-ground mangrove biomass carbon stock due to its relationship with LAI; (5) the relationship between mangrove LAI and below-ground parts, which are lower than the above-ground parts, thus affecting the relationship with mangrove reflectance; (6) the inability to perform carbon stock modelling at species level due to sensor limitations and mangrove forest complexity; (7) background reflectance and atmospheric path radiance that could not be fully minimized using image radiometric correction and transformation; and (8) spatial displacement between the mangroves' actual location in the field and the corresponding pixel in the image. This study shows that mangrove in the Karimunjawa and Kemujan islands stores a huge amount of carbon stock, which should be protected. From the resulting maps, total mangrove biomass carbon stock stored across the the Karimunjawa and Kemujan islands was estimated. There are potentially 120,546 tonnes C of mangrove

biomass carbon stock stored in these two islands, consisting of 96,482 tonnes C of AGC with a mean value of 21.64 kg C m^{-2} and 24,064 tonnes C of BGC with a mean value of 5.39 kg C m^{-2}. The availability of mangrove biomass carbon stock maps is beneficial for carrying out various management activities and is also very important for the resilience of mangrove to changing environments.

Acknowledgements

The authors would like to thank JAXA (Japan Aerospace Exploration Agency) and LAPAN for providing us with ALOS AVNIR-2 imagery of the Karimunjawa Islands and Muhammad Taufik Daryono, Muhammad Hafizt, and the staff at the Karimunjawa National Park for their assistance during field data collection.

Disclosure statement

No potential conflict of interest was reported by the authors.

Funding

The authors would like to thank CNRD (Center for Natural Resources and Development) and the Faculty of Geography, Universitas Gadjah Mada for funding the research.

References

Armstrong, R. A. 1993. "Remote Sensing of Submerged Vegetation Canopies for Biomass Estimation." *International Journal of Remote Sensing* 14: 621–627. doi:10.1080/01431169308904363.

Atzberger, C. 2004. "Object-Based Retrieval of Biophysical Canopy Variables Using Artificial Neural Nets and Radiative Transfer Models." *Remote Sensing of Environment* 93 (1–2): 53–67. doi:10.1016/j.rse.2004.06.016.

Bajracharya, S. 2008. "Community Carbon Forestry: Remote Sensing of Forest Carbon and Forest Degradation in Nepal." Masters Thesis. The Netherlands: International Institute for Geo-information Science and Earth Observatio, ITC.

Birth, G. S., and G. McVey. 1968. "Measuring the Color of Growing Turf with a Reflectance Spectrophotometer." *Agronomy Journal* 60: 640–643. doi:10.2134/agronj1968.00021962006000060016x.

Boonsong, K., S. Piyatiratitivorakul, and P. Patanaponpaiboon. 2003. "Potential Use of Mangrove Plantation as Constructed Wetland for Municipal Wastewater Treatment." *Water Science and Technology* 48: 257–266.

Bouillon, S., A. V. Borges, E. Castañeda-Moya, K. Diele, T. Dittmar, N. C. Duke, E. Kristensen, S. Y. Lee, C. Marchand, J. J. Middelburg, V. H. Rivera-Monroy, T. J. Smith, and R. R. Twilley. 2008. "Mangrove Production and Carbon Sinks: A Revision of Global Budget Estimates." *Global Biogeochemical Cycles* 22. doi:10.1029/2007GB003052.

Broge, N. H., and E. Leblanc. 2000. "Comparing Prediction Power and Stability of Broadband and Hyperspectral Vegetation Indices for Estimation of Green Leaf Area Index and Canopy Chlorophyll Density." *Remote Sensing of Environment* 76: 156–172. doi:10.1016/S0034-4257(00)00197-8.

Chave, J., C. Andalo, S. Brown, M. A. Cairns, J. Q. Chambers, D. Eamus, H. Fölster, F. Fromard, N. Higuchi, T. Kira, J.-P. Lescure, B. W. Nelson, H. Ogawa, H. Puig, B. Riéra, and T. Yamakura. 2005.

"Tree Allometry and Improved Estimation of Carbon Stocks and Balance in Tropical Forests." *Oecologia* 145: 87–99. doi:10.1007/s00442-005-0100-x.

Chen, X., L. Vierling, E. Rowell, and T. DeFelice. 2004. "Using Lidar and Effective LAI Data to Evaluate IKONOS and Landsat 7 ETM+ Vegetation Cover Estimates in a Ponderosa Pine Forest." *Remote Sensing of Environment* 91: 14–26. doi:10.1016/j.rse.2003.11.003.

Clark, M. L., D. A. Roberts, J. J. Ewel, and D. B. Clark. 2011. "Estimation of Tropical Rain Forest Aboveground Biomass with Small-Footprint Lidar and Hyperspectral Sensors." *Remote Sensing of Environment* 115: 2931–2942. doi:10.1016/j.rse.2010.08.029.

Clough, B. F., and K. Scott. 1989. "Allometric Relationships for Estimating Aboveground Biomass in Six Mangrove Species." *Forest Ecology Management* 27: 117–127. doi:10.1016/0378-1127(89)90034-0.

Comley, B. W. T., and K. A. McGuinness. 2005. "Above- and Below-Ground Biomass, and Allometry of Four Common Northern Australian Mangroves." *Australian Journal of Botany* 53: 431–436. doi:10.1071/BT04162.

Edwards, A. 2004. "Assesing Mangrove LAI using CASI Airborne Imagery." In *Bilko Tutorial on the Applications of Satellite and Airborne Image Data to Coastal Management*. Paris: UNESCO.

Eitel, J., D. Long, P. Gessler, and E. Hunt. 2008. "Combined Spectral Index to Improve Ground-Based Estimates of Nitrogen Status in Dryland Wheat." *Agronomy Journal* 100: 1694–1702. doi:10.2134/agronj2007.0362.

FAO. 2007. *The World's Mangroves 1980–2005*. FAO Forestry Paper 153. Rome: Food and Agriculture Organization of the United Nations.

Fatoyinbo, T., M. Simard, R. A. Washington-Allen, and H. H. Shugart. 2008. "Landscape-Scale Extent, Height, Biomass, and Carbon Estimation of Mozambique's Mangrove Forests with Landsat ETM+ and Shuttle Radar Topography Mission Elevation Data." *Journal for Geophysical Research-Biogeosciences* 113. doi:10.1029/2007JG000551.

Fatoyinbo, T. E., and A. H. Armstrong. 2010. "Remote Characterization of Biomass Measurements:Case Study of Mangrove Forests." In *Biomass*, edited by M. Momba and F. Bux. Croatia: Sciyo.

Gitelson, A. A., Y. J. Kaufman, R. Stark, and D. Rundquist. 2002. "Novel Algorithms for Remote Estimation of Vegetation Fraction." *Remote Sensing of Environment* 80: 76–87. doi:10.1016/S0034-4257(01)00289-9.

Granek, E., and B. I. Ruttenberg. 2008. "Changes in Biotic and Abiotic Processes following Mangrove Clearing." *Estuarine, Coastal and Shelf Science* 80: 555–562. doi:10.1016/j.ecss.2008.09.012.

Green, E. P., and P. J. Mumby. 2000. "Mapping Mangroves." In *Remote Sensing Handbook for Tropical Coastal Management*, edited by A. J. Edwards, 183–192. Paris: UNESCO.

Hadjimitsis, D. G., G. Papadavid, A. Agapiou, K. Themistocleous, M. G. Hadjimitsis, A. Retalis, S. Michaelides, N. Chrysoulakis, L. Toulios, and C. R. I. Clayton. 2010. "Atmospheric Correction for Satellite Remotely Sensed Data Intended for Agricultural Applications: Impact on Vegetation Indices." *Natural Hazards and Earth System Sciences* 10: 89–95. doi:10.5194/nhess-10-89-2010.

Hamdan, O., H. K. Aziz, and I. M. Hasmadi. 2014. "L-Band ALOS PALSAR for Biomass Estimation of Matang Mangroves, Malaysia." *Remote Sensing of Environment* 155: 69–78. doi:10.1016/j.rse.2014.04.029.

Huete, A., K. Didan, T. Miura, E. P. Rodriguez, X. Gao, and L. G. Ferreira. 2002. "Overview of the Radiometric and Biophysical Performance of the MODIS Vegetation Indices." *Remote Sensing of Environment* 83: 195–213. doi:10.1016/S0034-4257(02)00096-2.

Huete, A. R., G. Hua, J. Qi, A. Chehbouni, and W. J. Ven Leeuwem. 1992. "Normalization of Multidirectional Red and Near-infrared Reflectances with the SAVI." *Remote Sensing of Environment* 40: 1–20.

Huete, A. R., and H. Q. Liu. 1994. "An Error and Sensitivity Analysis of the Atmospheric and Soil-Correcting Variants of the NDVI for the MODIS-EOS." *IEEE Transactions on Geoscience and Remote Sensing* 32 (4): 897–905. doi:10.1109/36.298018.

Jiang, Z., A. R. Huete, K. Didan, and T. Miura. 2008. "Development of a Two-Band Enhanced Vegetation Index without a Blue Band." *Remote Sensing of Environment* 112 (10): 3833–3845. doi:10.1016/j.rse.2008.06.006.

Jusoff, K. 2006. "Individual Mangrove Species Identification and Mapping in Port Klang Using Airborne Hyperspectral Imaging." *Journal of Sustainability Science and Management* 1 (2): 27–36.

Kamal, M., and S. Phinn. 2011. "Hyperspectral Data for Mangrove Species Mapping:A Comparison of Pixel-Based and Object-Based Approach." *Remote Sensing* 3: 2222–2242. doi:10.3390/rs3102222.

Kattenborn, T., J. Maack, F. Faßnacht, F. Enßle, J. Ermert, and B. Koch. 2015. "Mapping Forest Biomass from Space – Fusion of Hyperspectral Eo1-Hyperion Data and Tandem-X and Worldview-2 Canopy Height Models." *International Journal of Applied Earth Observation and Geoinformation* 35: 359–367. doi:10.1016/j.jag.2014.10.008.

Kaufman, Y. J., and D. Tanre. 1992. "Atmospherically Resistant Vegetation Index (ARVI) for EOS-MODIS." *IEEE Transactions on Geoscience and Remote Sensing* 30 (2): 261–270. doi:10.1109/36.134076.

Kiage, L. M., and N. D. Walker. 2009. "Using NDVI from MODIS to Monitor Duckweed Bloom in Lake Maracaibo, Venezuela." *Water Resource Management* 23 (6): 1125–1135. doi:10.1007/s11269-008-9318-9.

Knyazikhin, Y., J. Glassy, J. L. Privette, Y. Tian, A. Lotsch, Y. Zhang, Y. Wang, Y. J. T. Morisette, P. Votava, R. B. Myneni, R. R. Nemani, and S. W. Running. 1999. *MODIS Leaf Area Index (LAI) and Fraction of Photosynthetically Active Radiation Absorbed by Vegetation (FPAR) Product (MOD15) Algorithm Theoretical Basis Document*. Greenbelt, MD: NASA Goddard Space Flight Center.

Komiyama, A., J. E. Ong, and S. Poungparn. 2008. "Allometry, Biomass, and Productivity of Mangrove Forests: A Review." *Aquatic Botany* 89: 128–137. doi:10.1016/j.aquabot.2007.12.006.

Komiyama, A., S. Poungparn, and S. Kato. 2005. "Common Allometric Equations for Estimating the Tree Weight of Mangroves." *Journal of Tropical Ecology* 21: 471–477. doi:10.1017/S0266467405002476.

Kovacs, J. M., X. Jiao, F. Flores-de-Santiago, C. Zhang, and F. Flores-Verdugo. 2013. "Assessing Relationships between Radarsat-2 C-Band and Structural Parameters of a Degraded Mangrove Forest." *International Journal of Remote Sensing* 34 (20): 7002–7019. doi:10.1080/01431161.2013.813090.

Kuenzer, C., A. Bluemel, S. Gebhardt, T. Vo Quoc, and S. Dech. 2011. "Remote Sensing of Mangrove Ecosystems: A Review." *Remote Sensing* 3: 878–928. doi:10.3390/rs3050878.

Laffoley, D. D., and G. Grimsditch. 2009. *The Management of Natural Coastal Carbon Sinks*, edited by G. Grimsditch. Gland: IUCN.

Latifi, H., F. Fassnacht, and B. Koch. 2012. "Forest Structure Modeling with Combined Airborne Hyperspectral and Lidar Data." *Remote Sensing of Environment* 121: 10–25. doi:10.1016/j.rse.2012.01.015.

Laurin, G. V., Q. Chen, J. A. Lindsell, D. A. Coomes, F. D. Frate, L. Guerriero, F. Pirotti, and R. Valentini. 2014. "Above Ground Biomass Estimation in an African Tropical Forest with Lidar and Hyperspectral Data." *ISPRS Journal of Photogrammetry and Remote Sensing* 89: 49–58. doi:10.1016/j.isprsjprs.2014.01.001.

Li, X., A. Gar-On Yeh, S. Wang, K. Liu, X. Liu, J. Qian, and X. Chen. 2007. "Regression and Analytical Models for Estimating Mangrove Wetland Biomass in South China Using Radarsat Images." *International Journal of Remote Sensing* 28 (24): 5567–5582. doi:10.1080/01431160701227638.

Liu, G. R., C. K. Liang, T. H. Kuo, T. H. Lin, and S. J. Huang. 2004. "Comparison of the NDVI, ARVI and AFRI Vegetation Index, Along with Their Relations with the AOD Using SPOT 4 Vegetation Data." *TAO* 15 (1): 15–31.

Lu, D., M. Batistella, and E. Moran. 2005. "Satellite Estimation of Aboveground Biomass and Impacts of Forest Stand Structure." *Photogrammetric Engineering & Remote Sensing* 71 (8): 967–974. doi:10.14358/PERS.71.8.967.

Lucas, R. M., A. L. Mitchell, A. Rosenqvist, C. Proisy, A. Melius, and C. Ticehurst. 2007. "The Potential of L-Band SAR for Quantifying Mangrove Characteristics and Change: Case Studies from the Tropics." *Aquatic Conservation: Marine and Freshwater Ecosystems* 17: 245–264. doi:10.1002/(ISSN)1099-0755.

Martawijaya, A., I. Kartasujana, K. Kadir, and S. A. Prawira. 1992. *Indonesia Wood Atlas*. 2 vols. Bogor: Department of Forestry, AFRD. Forest Product Research and Development Center.

Mougin, E., C. Proisy, G. Marty, F. Fromard, H. Puig, J. L. Betoulle, and J. P. Rudant. 1999. "Multifrequency and Multipolarization Radar Backscattering from Mangrove Forests." *IEEE Transactions on Geoscience and Remote Sensing* 37: 94–102. doi:10.1109/36.739128.

Murdiyarso, D., D. Donato, J. B. Kauffman, S. Kurnianto, M. Stidham, and M. Kanninen. 2009. *Carbon Storage in Mangrove and Peatland Ecosystem: A Preliminary Account from Plots in Indonesia*. Working Paper. Bogor: Center for International Forestry Research.

Myint, S. W., C. P. Giri, L. Wang, Z. Zhu, and S. C. Gillette. 2008. "Identifying Mangrove Species and Their Surrounding Land Use and Land Cover Classes Using an Object-Oriented Approach with a Lacunarity Spatial Measure." *GIScience & Remote Sensing* 45 (2): 188–208. doi:10.2747/1548-1603.45.2.188.

Nababan, M. G., Munasik, I. Yulianto, T. Kartawijaya, R. Prasetia, R. L. Ardiwijaya, S. T. Pardede, R. Sulisyati, Mulyadi, and Y. Syaifudin. 2010. *Status Ekosistem di Taman Nasional Karimunjawa: 2010*, 78. Bogor: Wildlife Conservation Society-Indonesia Program.

Nagelkerken, I., S. J. M. Blaber, S. Bouillon, P. Green, M. Haywood, L. G. Kirton, J.-O. Meynecke, J. Pawlik, H. M. Penrose, A. Sasekumar, and P. J. Somerfield. 2008. "The Habitat Function of Mangroves for Terrestrial and Marine Fauna: A Review." *Aquatic Botany* 89: 155–185. doi:10.1016/j.aquabot.2007.12.007.

Nellemann, C., E. Corcoran, C. M. Duarte, L. Valdes, C. De Young L. Fonseca, and G. Grimsditch. 2009. *Blue Carbon. A Rapid Response Assessment*, edited by G. Grimsditch. Arendal: United Nations Environment Programme, GRID-Arendal.

Ong, J. E. 2002. "The Hidden Costs of Mangrove Services: Use of Mangroves for Shrimp Aquaculture." In *International Science Roundtable for the Media*. Bali: ICSU, IGBP, IHDP, WCRP, DIVERSITAS, START.

Ong, J. E., W. K. Gong, and C. H. Wong. 2004. "Allometry and Partitioning of the Mangrove, Rhizophora Apiculata." *Forest Ecology Management* 188: 395–408. doi:10.1016/j.foreco.2003.08.002.

Oohata, S., and K. Shinozaki. 1979. "A Statistical Model of Plant Form - Further Analysis of the Pipe Model Theory." *Japanese Journal of Ecology* 29: 323–335.

Patel, N., and A. Majumdar. 2010. "Biomass Estimation of Shorea Robusta with Principal Component Analysis of Satellite Data." *Journal of Forestry Research* 21 (4): 469–474. doi:10.1007/s11676-010-0100-5.

Pinty, B., and M. M. Verstraete. 1992. "GEMI: A Non-Linear Index to Monitor Global Vegetation from Satellites." *Vegetatio* 101: 15–20. doi:10.1007/BF00031911.

Potithep, S., K. Nishida, R. Suzuki, S. Nagai, and Y. Yasuoka. 2009. *Comparison Between LAI Estimation Based Vegetation Index and MODIS LAI for Gross Primary Productivity Estimation, Deciduous Broadleaf Forest in Japan*. Fall Meeting 2009, San Francisco, CA: American Geophysical Union.

Poungparn, S., A. Komiyama, V. Intana, S. Piriyaota, T. Sangtiean, P. Tanapermpool, P. Patanaponpaiboon, and S. Kato. 2002. "A Quantitative Analysis on the Root System of A Mangrove, Xylocarpus Granatum Koenig." *Tropics* 12: 35–42. doi:10.3759/tropics.12.35.

Proisy, C., P. Couteron, and F. Fromard. 2007. "Predicting and Mapping Mangrove Biomass from Canopy Grain Analysis Using Fourier-Based Textural Ordination of IKONOS Images." *Remote Sensing of Environment* 109: 379–392. doi:10.1016/j.rse.2007.01.009.

Proisy, C., E. Mougin, F. Fromard, and M. A. Karam. 2000. "Interpretation of Polarimetric Radar Signatures of Mangrove Forests." *Remote Sensing of Environment* 71: 56–66. doi:10.1016/S0034-4257(99)00064-4.

Proisy, C., E. Mougin, F. Fromard, V. Trichon, and M. A. Karam. 2002. "On the Influence of Canopy Structure on the Radar Backscattering of Mangrove Forests." *International Journal of Remote Sensing* 23: 4197–4210. doi:10.1080/01431160110107725.

Richardson, A. J., and J. H. Everitt. 1992. "Using Spectral Vegetation Indices to Estimate Rangeland Productivity." *Geocarto International* 7: 63–69. doi:10.1080/10106049209354353.

Rouse, J. W., R. H. Haas, J. A. Schell, and D. W. Deering. 1973. "Monitoring Vegetation Systems in the Great Plains with ERTS." In *Third ERTS Symposium*, 309–317. Washington, DC: NASA.

Sakuno, Y., T. Kozu, Y. Tsuzuki, and T. Matsunaga. 2007. "Monitoring of Water Pollution and Aquatic Plants in the Coastal Lagoon Environments Using ALOS Data." In *The First Joint Pl Symposium of*

ALOS Data Nodes for ALOS Science Program in Kyoto, edited by T. Komatsu. Kyoto: Japan Aerospace Exploration Agency (JAXA).

Schlerf, M., C. Atzberger, and J. Hill. 2005. "Remote Sensing of Forest Biophysical Variables Using Hymap Imaging Spectrometer Data." *Remote Sensing of Environment* 95: 177–194. doi:10.1016/j.rse.2004.12.016.

Shinozaki, K., K. Yoda, K. Hozumi, and T. Kira. 1964. "A Quantitative Analysis of Plant Form—The Pipe Model Theory. II. Further Evidence of the Theory and Its Application in Forest Ecology." *Japanese Journal of Ecology* 14: 133–139.

Simard, M., V. H. Rivera-Monroy, J. E. Mancera-Pineda, E. Castañeda-Moya, and R. R. Twilley. 2008. "A Systematic Method for 3D Mapping of Mangrove Forests Based on Shuttle Radar Topography Mission Elevation Data, Icesat/GLAS Waveforms and Field Data: Application to Ciénaga Grande De Santa Marta, Colombia." *Remote Sensing of Environment, Earth Observations for Terrestrial Biodiversity and Ecosystems Special Issue* 112 (5): 2131–2144.

Simard, M., K. Zhang, V. H. Rivera-Monroy, M. S. Ross, P. L. Ruiz, E. Castañeda-Moya, R. R. Twilley, and E. Rodriguez. 2006. "Mapping Height and Biomass of Mangrove Forests in Everglades National Park with SRTM Elevation Data." *Photogrammetric Engineering & Remote Sensing* 72 (3): 299–311. doi:10.14358/PERS.72.3.299.

Thenkabail, P. S., N. Stucky, B. W. Griscom, M. S. Ashton, E. Enclona, J. Diels, and B. Van der Meer. 2002. "Biomass Estimations and Carbon Stock Calculations in the Oil Palm Plantations of African Derived Savannas using IKONOS Data." In *FIEOS 2002 Conference Proceedings*. Denver, CO: ISPRS.

Vaiphasa, C., A. K. Skidmore, and W. F. de Boer. 2006. "A Post-Classifier for Mangrove Mapping Using Ecological Data." *PandRS* 61 (1): 1–10.

Van der Meer, F., W. Bakker, K. Scholte, A. Skidmore, S. De Jong, J. Clevers, and G. Epema. 2000. "Vegetation Indices, Above Ground Biomass Estimates and The Red Edge From MERIS." In *International Archives of Photogrammetry and Remote Sensing*, XXXIII vols, edited by G. Remetey-Fülöpp, J. Clevers, and K. J. Beek. Part B7. Amsterdam: International Society of Photogrammetry and Remote Sensing (ISPRS).

Viña, A., and A. A. Gitelson. 2011. "Sensitivity to Foliar Anthocyanin Content of Vegetation Indices Using Green Reflectance." *IEEE Geoscience and Remote Sensing Letters* 8 (3): 464–468. doi:10.1109/LGRS.2010.2086430.

Wamunyima, S. 2005. "Estimating Fresh Grass Biomass at Landscape Level Using Hyperspectral Remote Sensing." Master Thesis. Enschede, The Netherlands: International Institute for Geo-Information Science and Earth Observation (ITC).

Wicaksono, P., P. Danoedoro, Hartono, U. Nehren, and L. Ribbe. 2011. "Preliminary Work of Mangrove Ecosystem Carbon Stock Mapping in Small Island Using Remote Sensing: Above and below Ground Carbon Stock Mapping on Medium Resolution Satellite Image." In *Proceedings of SPIE 8174, Remote Sensing for Agriculture, Ecosystems, and Hydrology XIII, 81741B*, edited by C. M. U. Neale and A. Maltese. Prague: SPIE Remote Sensing.

Williams, G. J. 2012. "Estimating Chlorophyll Content in a Mangrove Forest Using a Neighbourhood Based Inversion Approach." Masters Thesis. Twente, The Netherlands: Geo-information Science and Earth Observation for Environmental Modelling and Management, University of Twente, Faculty ITC.

Wong, F. K., and T. Fung. 2014. "Combining EO-1 Hyperion and Envisat ASAR Data for Mangrove Species Classification in Mai Po Ramsar Site, Hong Kong." *International Journal of Remote Sensing* 35 (23): 7828–7856. doi:10.1080/01431161.2014.978034.

Woodhouse, I. H., E. T. A. Mitchard, M. Brolly, D. Maniatis, and C. M. Ryan. 2012. "Radar Backscatter Is Not a 'Direct Measure' of Forest Biomass." *Nature Climate Change* 2: 556–557. doi:10.1038/nclimate1601.

Worldagroforestry. 2013. *Wood Density Database*. Accessed March 28 2013. http://db.worldagroforestry.org/wd.

Wu, Y., A. Chung, N. F. Y. Tam, N. Pi, and M. H. Wong. 2008. "Constructed Mangrove Wetland as Secondary Treatment System for Municipal Wastewater." *Ecological Engineering* 34: 137–146. doi:10.1016/j.ecoleng.2008.07.010.